IFIN-HH UPB ELI-NP

UNIVERSITY POLITEHNICA OF BUCHAREST

Doctoral School of Engineering and Applications of Lasers and Accelerators

DOCTORAL THESIS

Summary

Optimization of nuclear reactions as a source of radioisotopes production of medical interest

Supervisor
CS I. Dr. Călin Alexandru UR

Phd. Student
Ionela Simona ILIE (BĂRUȚĂ)

Bucharest 2022

Acknowledgements

First, I wish to express my gratitude to my supervisor, Mr. Dr. Calin Alexandru Ur for providing me the opportunity to be part of this Ph.D. program. I want to thank him for his continuous patience, for his detailed and constructive comments and support of my research, and for careful reading and correction of this work.

Special thanks are owed to Ms. Dr. Maria Sahagia and Mr. Prof. Octavian Sima for their kind support, encouragement, and patience to discuss the scientific problems of my work. All my thanks for their valuable suggestions, and continuous encouragement.

Special thanks to Ms. Dr. Dana Niculae for her help in solving numerous small and big problems alike, for her patience, encouragement feelings, progressive discussion, friendly guidance during several years, and for her keeping the study plan achievable.

Many thanks to my colleagues and co-authors from CCR and GSD team, for their help, support, and useful discussions.

The acknowledgments section is not enough to express how much I appreciate their support.

Table of contents

List of Figures

List of Tables

List of Acronyms

A	Amplifier
ADC	Analog to Digital Converter
CCR	Radiopharmaceutical Research Center
CT	Computer Tomography
EDS	Electro-Deposition
ELI-NP	Extreme Light Infrastructure – Nuclear Physics
EOB	End of Bombardment
HV	Higach-Voltage
HPGe	High-Purity Germanium
ICS	Inverse Compton Scattering
IFIN-HH	Horia Hulubei National Institute for R&D in Physics and Nuclear Engineering
MCA	Multi-Channel Analyzer
PA	Preamplifier
PAT	Total Absorption Peak
PET	Positron Emission Tomography
PTS	Pneumatic Transfer System
SPECT	Single-Photon Emission Computed Tomography
TADDEO-PRF	Purification Module
VEGA	Variable Energy Gamma System

Keywords: *Radioisotopes production, nuclear and photonuclear reactions, HPGe detectors, simulation vs experiment*

Introduction

Methods of obtaining medical radioisotopes by irradiating different types of targets using charged particles at cyclotron, is an important way to produce them, depending on the characteristics of the targets and the technical parameters of the cyclotron.

In this work, the emphasis was on methods of optimizing nuclear reactions as a source of obtaining medical radioisotopes, with a special focus on the obtaining and characterizing a ^{64}Cu based radiopharmaceutical, as well as investigating other routes of radioisotope production, highlighting the advantages and disadvantages of using different production methods.

The first chapter presents the theoretical aspects necessary to understand the methods of obtaining isotopes, starting from the notions of nuclear physics, radioactivity, photon interaction with matter, followed by a brief description of the methods of detection and measurement of nuclear radiation. The technique of positron emission tomography (PET) and single-photon emission tomography (SPECT) is also presented in this work.

The second chapter contains information about the semiconductor HPGe detectors used in this work for quantitative and qualitative analyzes of radioisotopes obtained from cyclotron irradiation.

Chapter three details the operating principle of the TR-19 cyclotron and the obtaining of cyclotron radionuclides involving the use of the automatic solid target system.

Chapter four focuses on the production of the ^{64}Cu radioisotope by irradiating of ^{64}Ni enriched targets at cyclotron. In the first part of the chapter are described the simulations performed in Geant4 for the production of ^{64}Cu radioisotope by using different irradiation parameters (time, current, energy of the proton beam, targets with different degrees of enrichment). The second part of chapter five describes the experiment performed at TR-19 cyclotron for the validation of the simulation results performed to obtain the ^{64}Cu radioisotope. Also, this chapter are described the steps and methods for characterizing the solution obtained after the irradiation of the ^{64}Ni target and purification steps. The last part of the chapter aims to evaluate the quality of ^{64}Cu radionuclide obtained using the nuclear reaction (p, n) at the TR-19 cyclotron and the automated solid target system by using the ^{64}Cu solution as a radiotracer for PET / CT imaging.

Chapter five covers the methods of obtaining radioisotopes of medical interest using photonuclear reactions, considering the significant evolution of the characteristics of gamma beams obtained by Inverse Compton Scattering of laser beams on relativistic electron beams, and also taking into account that such system is being implemented at the Extreme Light Infrastructure - Nuclear Physics (ELI-NP) in Romania. The Variable Energy Gamma-ray system (VEGA) will generate monochromatic gamma-ray beams and will have special characteristics in terms of small relative bandwidth ($\leq 0.5\%$), high spectral density (≥ 500 photons / s / eV) and

will present a high degree of linear polarization (≥ 95%). Taking into account these characteristics of the gamma beams, the methods for obtaining ^{64}Cu radionuclide were investigated by using the photonuclear reaction (γ, n) using ^{65}Cu targets and of ^{99}Mo using ^{100}Mo targets.

Chapter six presents the results and discussions regarding the obtaining of the ^{64}Cu radioisotope by using both nuclear photonuclear reactions, being presented the advantages and disadvantages of using the two production methods.

The thesis concludes with the general conclusions of the experiments and simulations performed and with the presentation of the perspectives for further development.

1 Theoretical background

1.1 Introductory notions

The introductory notions briefly presented in this chapter are necessary to understand the methods of obtaining isotopes, starting from the notions of nuclear physics, radioactivity, decay modes, photon interaction with matter, followed by a brief description of the methods of detection and measurement of nuclear radiation.

1.1.1 Radioactivity

Radioactivity is a physical phenomenon by which an unstable nucleus, called radionuclide (radioisotope), spontaneously transforms (decays) into a more stable one, releasing energy in the form of radiation (alpha, beta, gamma).

Radioactive substances emit three types of radiation that are, in the ascending order of their penetrating power: alpha radiation (α), beta radiation (β^+, β^-) and gamma radiation (γ) directly from nucleus.

In addition to this type of radiations, the following ones are also emitted in the process of radioactive decay: neutrinos and antineutrinos that accompany β+ and β- decays, respectively and radiations emitted in the process of atomic relaxation by transitions between electronic shells: X-rays, Auger and Koster Kroning electrons, internal conversion electrons, subsequent to radioactive decay processes.

The nuclei that emit alpha or beta radiation, remain in most cases, in an excited energetic state. Spontaneous or delayed emission of gamma radiation occurs as a result of de-excitation of the nuclei to a lower excited state or to the ground state, following the decay processes α, β or electron capture.

Internal conversion is a competing process to gamma-ray decay and occurs when an excited nucleus interacts electromagnetically with an orbital electron and ejects it.

The radionuclide ^{64}Cu decays by three modes, which combines electron capture, β-, and β+ decays and also results in Auger electron emission with therapeutic potential, being in this way the most versatile of all the copper radionuclides.

Radioactive decay occurs according to a statistical law, so that the number of nuclei dN that decay in the time interval dt and the number of nuclei N, which have not yet decayed by the time t.

The activity of a radioactive source is given by the number of nuclei that decay in the unit of time (number of decays per second), and it is measured in Becquerel [Bq], 1 Bq= 1 s^{-1}.

1.1.2 Nuclear reactions

Radioisotopes used in medical applications are produced by using different types of accelerators or by using nuclear reactors, both production routes involving nuclear reactions.

The nuclear reaction is a process in which two nuclei, or a nucleus and an external subatomic particle, collide to produce one or more new nuclides. Thus, a nuclear reaction causes a transformation of at least one nuclide to another. [1].

The classification of nuclear reactions is done according to the following criteria, depending on the quantum states of the interaction partners in the initial and final state, on the nature of the projectile, on the mass number.

The value by which the intensity of a nuclear reaction is characterized is called the reaction cross-section.

The reactions produced by photons, photonuclear reactions, although known for decades, have been much less used. This is due to the fact that there was no gamma photon beam with intensity and energy parameters suitable to the study of nuclear structure. Photons provide a precise way to study nuclear properties and processes.

Photonuclear reactions have been used since the advent of very intense γ sources developed by using the Compton back-scattering of laser light from high energy electron bunches [2].

The most interesting cases for isotope production are photoneutron and photoproton reactions.

1.1.3 Interaction of gamma radiation with matter

The gamma-rays interact with detectors by three major processes: photoelectric effect, Compton effect, and pair production process. In the photoelectric effect, the gamma-ray loses all of its energy in one interaction. The probability for this process depends very strongly on gamma-ray energy and atomic number Z. In the Compton effect, the gamma-ray loses only part of its energy in one interaction. The effect of pair production is a threshold process. The condition of this process to take place is that the energy of the photon must be at least equal to twice the energy corresponding to the rest mass energy of the electron (1.022 MeV).

1.1.4 Detection and measurements of nuclear radiation

The nuclear radiations are detected using systems that measure the amount or number of ionization or excitation events produced in a sensitive volume of a detector.

The radiation detector usually consists of the detection body and the system for recording the effect produced by the particle, to amplify and process the obtained signal.

The types of detectors used to detect nuclear radiation are gaseous detectors (ionization chambers, proportional counters and Geiger-Muller counters), scintillation detectors coupled with photomultipliers and semiconductor detectors.

1.2 Notions of Nuclear Medicine

Nuclear medicine is a branch of medicine that uses radiopharmaceutical products to diagnose and treat diseases in a non-invasive and painless manner.

Radioisotopes are used in nuclear medicine for diagnostic and therapeutic purposes being combined with compounds or biomolecules to form radiopharmaceuticals. Radiopharmaceuticals are introduced into the body of the patient through injection, ingestion or inhalation, and then can be targeted to particular organs or cellular receptors.

1.2.1 The availability of medical radioisotopes and their characteristics

In the present time, most of the radioisotopes of medical interest are produced involving nuclear reactions performed using particle accelerators, nuclear reactions using reactors, generators, and also photonuclear reactions represents an alternative route to produce this type of radioisotopes used in diagnostic and therapy procedures.

In this work we will be focused on the production of radioisotopes with charged-particles reactions and photonuclear reactions.

The selection of the radioisotopes to be used in diagnostic and therapy procedures is a very important step, depending on their usefulness and purpose.

Among the properties that a radioisotope must have are: the type of radiation emitted (it must be suitable for the proposed medical purpose, otherwise it may increase the dose), the half-life (suitable for the desired type of application), radionuclide and radiochemical purity, high biological affinity, feasible and safe production method, and also the production method to be cost-effective.

1.2.2 Medical imaging using SPECT and PET techniques

The most common methods used in nuclear imaging are Positron Emission Tomography, usually combined with a Computer Tomography, PET/CT, and Single-Photon Emission Computed Tomography (SPECT), their choice being made according to the used radionuclide [3].

SPECT is an imaging technique that is based on the detection of single photons using a pharmaceutical compound labeled with a gamma radiation emitting radioisotope that is injected into the patient/animal [4]. The most widely used radionuclides in SPECT imaging are ^{67}Ga, ^{99m}Tc, ^{111}In, ^{123,131}I, ^{201}Tl.

PET procedures involve short half-life isotopes generated from a cyclotron and labeled with biological molecules which are injected into patients. The most widely used radionuclides in PET imaging are: ^{11}C, ^{18}F, ^{60,61,64}Cu, ^{66,68}Ga, ^{124}I, ^{52}Mn

2 Experimental equipment and measurements by using high-purity germanium (HPGe) detectors

2.1 Semiconductor detectors

The use of semiconductor germanium detectors in gamma-ray spectrometry has many applications, being the most widely used procedures for the identification and quantification of unknown gamma-ray emitting radionuclides, analysis of the radioactive material present in the irradiated target and for example the analysis of radioactive products obtained by different methods, such as proton irradiation, in terms of activity and radionuclide purity determination.

Given that the vast majority of radioisotopes of medical interest are emitters of gamma radiation with different energies and intensities, germanium detectors are among the most suitable for characterizing these radioisotopes given the high energy resolution of the detectors.

The main feature of the HPGe semiconductor detectors is the high energy resolution, because to produce an electron-hole pair requires an energy of only 3 eV of energy stored in the detector, which results in a good statistic of the number of electron-hole pairs created and an excellent resolution.

The normal operation of the germanium detectors must ensure several conditions, including the cooling of the detector with liquid nitrogen (77 K), constant temperature and humidity and also suitable window for the energy of the photons to be measured.

2.2 Gamma-ray spectrometry with High Purity Germanium (HPGe) detectors

Using gamma-ray spectrometry, the gamma radiations present in the analyzed samples are determined quantitatively and qualitatively.

The detection of gamma radiation is based on the three main interaction processes: photoelectric effect, Compton scattering and the production of positron - electron pairs.

Photons interact with the sensitive volume of the detector, generating a current pulse that is picked up by a preamplifier, transforming it into a voltage signal, which it is then transmitted to an amplifier that forms and amplifies it.

A standard gamma-ray spectrometry set-up consists of HPGe semiconductor detector with preamplifier (PA) and high voltage (HV) source, amplifier (A), multichannel analyzer (MCA) with analog-to-digital converter (ADC) and appropriate processing and storage software [5] [6].

2.3 HPGe detectors used in this work

Two types of semiconductors HPGe detectors with different relative efficiencies were used for the experiments presented in this work

One of the HPGe detector used for the measurements is a HPGe detector with 25% relative efficiency, placed in the Spectrometry Laboratory for Radiopharmaceutical Research Center (CCR) at Horia Hulubei - National Institute for R&D in Physics and Nuclear Engineering (IFIN-HH). The detector is used for radionuclide identifications, activity and radionuclide purity determinations.

The other detector used in the measurements that will be presented in the following is a HPGe detector with a relative efficiency of 150% from the Spectroscopy Laboratory of ELI-NP. The high relative efficiency of this detector makes it suitable for use in in-beam measurements at high gamma-ray energies.

2.4 Calibration of HPGe detectors

The energy and efficiency calibrations of the spectrometric system allow the quantitative and qualitative analysis of gamma radiation emissions from the analyzed samples.

The energy calibration determines the energy values of gamma radiation emitted by a particular sample, the identification of radionuclides present in that sample, while after efficiency calibration of the system can be calculated the values of radionuclide activities present in the sample and also the associated uncertainties [7].

2.4.1 Energy calibration

The energy calibration of the detectors consists in establishing a relationship between the energy of the incident photons captured by the detector and the energy channel in which the pulses are recorded [8]. To establish this relationship, the spectrum of a radioactive source that emits radiation with well-known energies is measured.

2.4.2 Efficiency calibration

After identifying the gamma emitting radionuclides present in the sample, the next step is to calculate the activity of the identified radionuclides. To perform this step the spectrometric system must be calibrated in efficiency. This calibration consists in establishing a function that describes the energy dependence of the total absorption efficiency.

2.5 Determination of activity by using gamma-ray spectrometry method

The activity of a radioactive source is given by the number of nuclei that decay in the unit of time (number of decays per second), and it is measured in Becquerel [Bq].

From a metrological point of view, the measurement of the activity of a radionuclide is not sufficient, being necessary the associated uncertainty, which depends mainly on the uncertainty of the net area and that corresponding to the detection efficiency value.

Usually, the efficiency of the detectors is assessed by making well controlled measurements of standard gamma-ray sources, measured by absolute or relative methods in a radionuclide metrology laboratory, with an accurately known and certified activity, but may appear situations when the activity of the source is unknown. In such situations an important alternative is to firstly determine the activity of some simple decay scheme source by using only the spectral data and secondly to determine the efficiency of the detector.

In order to determine the unknown activity of a radioactive source on the basis of gamma-ray spectrometry, the sum-peak method, which is a primary activity measurement procedure, can be applied for specific nuclides.

The method allows for absolute activity measurements for point sources containing radionuclides with simple decay scheme similar to ^{60}Co emitting two coincident gamma-ray photons.

The working principle of this method is that when two photons interact with a detector in a time interval shorter than the resolving time, each transferring the full energy to the detector, the detector response is proportional to the total deposited energy and a sum-peak appears in the spectrum. The count rate in the sum-peak, together with the count rates from the characteristic peaks of ^{60}Co source and from the integral spectrum can be used for activity assessment.

The advantage of this method is that the activity of gamma cascade emitting sources can be determined based only on the use of measured spectra, without knowledge of the detector efficiencies. Most commonly, the method is applied to point-like sources measured in a close geometry, which improves the statistics of the counts in the sum-peak.

This method were applied to determine the activity of a calibrated point source of ^{60}Co by using the coaxial HPGe detector with a relative efficiency of 150% from Spectroscopy Laboratory, ELI-NP.

The obtained results emphasized that the activity of ^{60}Co could be calibrated with uncertainty not exceeding 5% by using a single HPGe detector and the sum-peak method by taking into considerations the corrections due to angular correlations and the pulse pile-up, although this uncertainty is higher than in the case of beta-gamma coincidence method, with an uncertainty less than 1%.

Based on these results, an article was published in Romanian Reports in Physics 71, 211 (2019) [9].

3 Cyclotron operating principle and production of radionuclides

The cyclotrons are the most used particle accelerators to produce radionuclides of medical interest compared to other particle accelerators such as linear accelerators.

The principle of operation of a cyclotron is to accelerate a beam of charged particles using a high frequency RF field that is applied between two "D" electrodes, called "dees" inside a vacuum chamber. Charged particles can be positive ions (proton, deuteron, α particle) or negative ions (negatively charged hydrogen atom, H^-).

Irradiating the target material, the particles interact with the target nuclei and nuclear reactions appear. The incident particle can be totally absorbed, depositing all its energy, or it can leave the nucleus after interaction with one or more nucleons, leaving some of its energy behind. In both cases, an excited nucleus is formed, and the excitation energy is dissipated by the emission of protons or neutrons. To prevent the generation of radionuclides impurities, the target material for irradiation must be pure and ideally mono-isotopic, or at least isotopically enriched.

Chemical processes such as solvent extraction, chromatography, ion exchange, are used to separate radionuclides from the target material [10]. Since cyclotron-produced radionuclides are neutron-deficient they are decaying through β^+ emission or electron capture.

The radionuclides that differ from the target nuclides have no stable atoms and are referred to as carrier-free radionuclides.

3.1 Description of the TR-19 Cyclotron

The TR-19 cyclotron, located in CCR, accelerates negative hydrogen ions (H^-), on a vertically arranged plane, having an external ion source [11].

Two extracted beams are positioned on two opposite sides of the cyclotron, being configured as follow:

- On side 1, the extracted beam is passed through a deflector magnetic system that allows the selection of two transport paths:
    - **the horizontal beam line** with a length of 6 m which transfers the proton beam from the cyclotron bunker to the experimental hall.
    - **the secondary beam line**, mounted on a 26° slope down extension proton beam line of the cyclotron which is intended for irradiations on solid targets.
- On side 2 there is a target selector head with a capacity to install a maximum of four targets (reaction chambers). The system is essentially a motorized device that allows the automatic alignment of the proton beam with any of the four targets.

The extraction energy can be varied in the 14-19 MeV range, with a 0.1 MeV energy step. The maximum available current on the horizontal beam line is 300 μA, depending on the maximum current allowed by the reaction chamber used. The intensity of the proton current in

the secondary beam line is limited at a maximum of 40 μA by the design of the solid target irradiation system

The TR-19 cyclotron, providing accelerated protons with energies ranging from 14 to 19 MeV, can be used to produce the PET radioisotopes ^{64}Cu, ^{18}F, and ^{15}O, as well as other medical radioisotopes previously produced using other methods (^{99m}Tc and ^{68}Ga) [12].

One of the aims of this thesis work was to study the production of ^{64}Cu radioisotope via nuclear reaction ^{64}Ni(p,n)^{64}Cu by using the TR-19 cyclotron and the automated solid target system as it will be discussed in the following.

4 Production of ^{64}Cu medical radioisotope by proton irradiation of enriched ^{64}Nickel target

Nowadays, many different medical radioisotopes, each with unique physical and chemical properties, play significant roles in nuclear medicine applications. The selection criteria of the radioisotopes for medical use must be based on the physical data about the radionuclide, its production and chemistry.

^{64}Cu is the most versatile of all the copper radionuclides owing to its unique decay scheme, which combines electron capture, β-, and β+ decays and also results in Auger electron emission with therapeutic potential. Its half-life of 12.7 h is long enough for radiopharmaceutical synthesis of many compounds and the properties make it suitable for applications in both PET imaging and targeted radiotherapy.

The production of copper radionuclides, using different cyclotrons, target supports, and enriched starting materials has been studied and the results are reported in relevant literature [13, 14, 15]. The demand for ^{64}Cu worldwide increased as it was proven that its production with high yield and high specific activities using typical “medical” cyclotrons (proton energy ranging from 11 to 18 MeV) was feasible in routine conditions [16].

Among the investigated production nuclear reactions, ^{64}Ni(p,n)^{64}Cu is the most widely employed, due to the high production yield for the ^{64}Cu at low energy protons [17, 18]. This production route bears the advantage of fewer side reactions inducing radionuclide impurities into the final product [19, 20, 21]. Taking into consideration the disadvantage of this process consisting in the use of expensive enriched ^{64}Ni targets, it is essential to optimize production by maximizing the yield by performing simulations before to start the experiments.

4.1 Geant4 simulations for production of ^{64}Cu

The Monte-Carlo simulation codes was used prior to experiments for the optimization of radioisotopes production by modification of the input parameters such as thickness of the target, as well as target materials that role as a critical assessing the yield for isotope production.

We used Geant4 for simulations of the nuclear reactions for ^{64}Cu production via a solid target irradiation system, installed on the extension of the proton beamline of a TR-19 cyclotron.

The output results from the simulation consist in the file providing a list of radioisotopes produced during the irradiation of the target. For each isotope it contains name of the isotope, number of isotopes created during the simulation, decay constant, half-life time, activity of the isotope at the end of the beam (mCi).

The simulation was modified to emulate the particular geometry of the solid target irradiation station, which is a tube surrounded by aluminum, a degrader foil made of aluminum, the volume of helium between the degrader foil and the target. The transfer of the target to/from cyclotron irradiation station is done pneumatically through a flexible tube, which connects the electrodeposition and dissolution module, to the irradiation station.

According to the ^{64}Ni(p,n)^{64}Cu reaction cross-section, the highest yield of it is expected at 11.66 MeV incident proton beam energy.

Taking into account the fact that the energy range of the TR-19 cyclotron is between 14-19 MeV, and the maximum of the reaction cross section is around 11.6 MeV for the ^{64}Ni (p,n) ^{64}Cu nuclear reaction, it is necessary to degrade the energy of the cyclotron from 14 MeV to 11.6 MeV by using de aluminum foil.

Several simulations were performed to degrade the energy of the TR-19 cyclotron by varying the thickness of the aluminum foil: no foil, 200 μm, 320 μm and 400 μm were considered, respectively.

In Figure 1, the ^{64}Cu activity at the end of bombardment (EOB) is represented as a function of energy, depending on the thickness of the aluminum foil degrader, at constant irradiation parameters 4 h and 20 μA (80 μAh). The simulation results showed that the optimal thickness of the aluminum foil is 320 μm, for which the estimated activity increased from 177 mCi (6.6 GBq) (2.2 mCi/μAh) without Al foil to about 277 mCi (10.3 GBq) (3.5 mCi/μAh).

The yield and activity values were calculated according to the formulas used in the validated simulation code [22] [23]. The final value of the specific activity is given in $mCi \cdot \mu A^{-1} \cdot h^{-1}$, calculated by dividing the activity by the current of the proton beam and the time of irradiation. In the simulations, the values of σ_i (E) were taken from ENDF database.

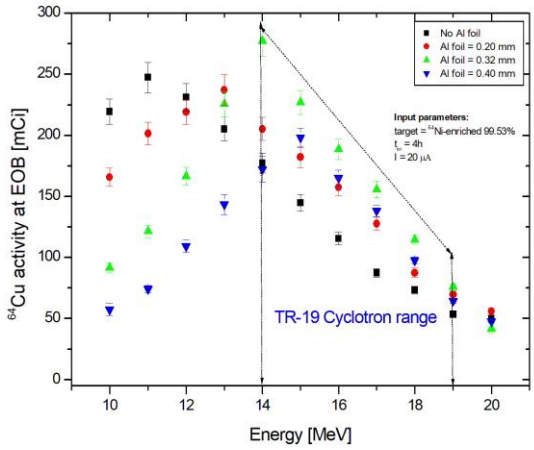

Figure 1. Dependence of ^{64}Cu activity at EOB on proton energy for Al foils with various thicknesses.

To optimize the input parameters used in irradiation for obtaining the highest possible value of ^{64}Cu radioisotope activity, in the simulation the parameters such as irradiation time and proton beam current were varied. The results showed that for an irradiation time of 4 h and a beam current of 25 μA t, the resulting activity is 365 mCi (3.65 mCi / μAh), with 12% more than in the case of irradiation with a proton beam current of 20 μA. It is also observed that using an irradiation current of 20 μA, but a time of 6 h the resulting activity is 448 mCi (3.7 mCi/μAh). The simulation input parameters referred also to different levels of enrichment of the ^{64}Ni targets, as presented in Table 1.

Table 1. Isotopic composition of enriched ^{64}Ni target.

Isotope	**^{64}Ni target (95%)**	**^{64}Ni target (99.53%)**
^{58}Ni	2.6	0.04
^{60}Ni	1.72	0.02
^{61}Ni	0.15	0.01
^{62}Ni	0.53	0.40
^{64}Ni	95	99.53

On 99.53% ^{64}Ni enriched target, the maximum activity at EOB for ^{64}Cu radioisotope obtained from simulation was around 277 mCi (3.5 mCi/μAh), for the following input parameters: current intensity 20 μA, irradiation time 4 h and the thickness of Al foil 320 μm. In the case of 95% ^{64}Ni enriched target, the maximum activity at EOB for ^{64}Cu was around 255 mCi (3.2 mCi/μAh), with the same input parameters.

Figure 2 presents the comparison between the ^{64}Cu activity at EOB by using different enrichment levels of target material (^{64}Ni).

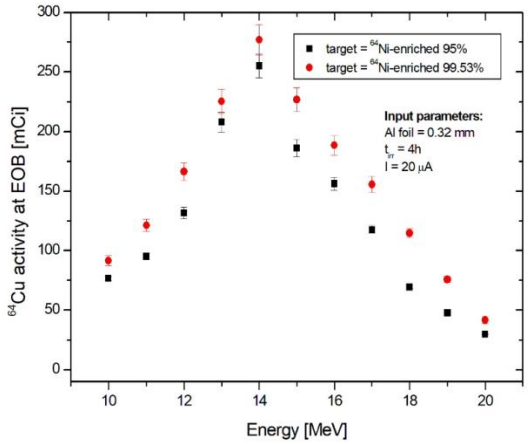

Figure 2. ^{64}Cu activity at EOB by using different enrichment of ^{64}Ni targets.

The purpose of the simulations performed before performing the experiments was to optimize the input parameters, to maximize the production yield for the ^{64}Cu radioisotope and implicitly to obtain a higher activity.

The parameters used in the simulation were implemented in the experiments, aiming also to compare the results and to validate the simulation results through experimental data.

4.2 Experimental production of ^{64}Cu by using ^{64}Ni enriched target to TR-19 cyclotron and automated solid target system

The experimental work was performed at CCR The ^{64}Cu radioisotope was produced via the nuclear reaction ^{64}Ni(p,n)^{64}Cu by using the TR-19 cyclotron and the automated solid target system (ALCEO, Comecer S.p.A, Italy) **[24]**.

The automated solid target system employed in the process includes modules for electro-deposition (EDS), pneumatic transfer system (PTS) and purification (Taddeo-PRF).

The automatic operations of the EDS module consist in storing a maximum of three targets, deposition of the isotope to be irradiated inside the target shuttle, sending the irradiated target to the cyclotron through a corrugated tube, recovering the irradiated target and dissolving the irradiated isotope.

The PTS system (irradiation unit) is fixed directly to the cyclotron and connected to the module through the transfer tube having the function of receiving and correctly positioning the target on the same axis as the cyclotron beam line. Another function of the PTS is to send the irradiated targets back to the EDS module at the end of the irradiation.

The TADEO-PRF module is a compact system designed to automatically purify ^{64}Cu. The module is based on "disposable cassette" technology, such as all components that come in contact with the radioactive product or various reagents are part of the sterile disposable kit. This

construction eliminates the step of decontaminating the module at the end of the synthesis and avoids problems that may arise related to the sterility of the product.

The target is produced in the EDS module, which contains the necessary parts and controls for electro-deposition process. The removable part of the electrolytic cell is the so-called shuttle, which is an aluminum cylinder with 28 mm diameter and 35 mm length, housing a platinum cup that represents the base for ^{64}Ni electro-deposition. The platinum cup is placed on the gold cathode. The anode consisting in a platinum wire is placed inside a plastic tube, connected to the vial containing the ^{64}Ni solution.

A mass of 47.47 mg of highly enriched ^{64}Ni (99.53 %), metallic form, were dissolved in HNO_3 (60%) resulting nickel nitrate, $^{64}Ni(NO_3)_2$. The pH was adjusted to 9.30 with NH_4Cl/NH_4OH buffer solution. The electroplating was performed by recirculation of the ^{64}Ni solution at 2-3 mL/min flow rate, operating voltage of 2.7-2.9 V and a current of 37 mA for about 15 hours, until the color changes from specific blue to colorless, indicating the completion of electro-deposition. At the end of electro-deposition step, resulted a compact target, without visible stalagmites or cracks, deposited in the center of the platinum cup in a circular shape with 6 mm diameter and 600 μm thickness.

After electroplating, the target is transferred from EDS to the irradiation unit through a flexible pipe, using a pneumatic system. Proton energy was degraded from 14 MeV to 11.7 MeV with an Al foil of 320 μm thickness, based on the simulation results presented above.
The target was irradiated for 4 h at 20 μA beam intensity.

Before running the beam on the target, the beam profile was assessed by the "classical" paper burn test, which provided information about the beam diameter and shape.

The shuttle was delivered back to the EDS unit, where the irradiated target was dissolved with HCl 6M.

To eliminate the metallic contaminants (Co, Ni, Fe. Zn), the solution containing $^{64}CuCl_2$ was purified by cation exchange technique in the purification module. The acidic solution obtained after the dissolution of the target in HCl was transferred to the purifying column loaded with 9 g of AG1-X8 resin. The nickel of the target was recovered with 40 mL of HCl 6M in chloride form ($NiCl_2$,) followed by separation of metallic impurities by washing with HCl 4M. ^{64}Cu was eluted with HCl 0.5 M in the form of $^{64}CuCl_2$.

The parameters of the experimental work and simulation are presented in Table 2.

Table 2. Input and output parameters used in simulation and experiment to produce ^{64}Cu

	Input Parameters	Simulation	Experiment
Beam parameters	Incident Energy	14 MeV, degraded to 11.66 MeV using 320 μm Al foil	14 MeV (degraded with 320 μm Al foil) to 11.66 MeV
	Current	20 μA	20 μA
	Irradiation time	4h	4h
Target parameters	Material	Enriched ^{64}Ni (99.53%)	Enriched ^{64}Ni (99.53%)
	Mass after electrodeposition	47.4 mg	47.4 mg
	Electrodeposition yield	-	99.83 %
	Thickness	600 μm	~ 600 μm
	Diameter	6 mm	~ 6 mm
Results	Activity at EOB	**277 mCi (10.3 GBq)**	**236 mCi (8.73 GBq)**

A good correlation of the simulation results with the experimental data was observed, the estimated activity in the given conditions, of 277 mCi, was well replicated by the 236 mCi experimentally obtained. The difference of only 14% is expected and acceptable; it can be attributed to the process losses of activity, mainly in the purification step, and also contain the uncertainty on the cross-sections values used, geometry and unevenly distribution of the mass in the real target.

Also, in the next future are proposed experiments where the parameters such as the irradiation current and the irradiation time will be varied, following that the experimental results will be compared with those obtained following the simulations presented above.

4.2.1 Characterization of the $^{64}CuCl_2$ solution by using gamma-ray spectrometry method

When irradiating ^{64}Ni enriched target with protons, various radioisotopes can be produced by side nuclear reaction on the metallic impurities contained in the target material. Radionuclide impurities can originate from radionuclides produced during the target irradiation and may also be the result of target material impurities. Before initial use of PET radionuclides in the synthesis of radiolabeled compounds, the radionuclide impurities must be determined.

The main radioisotope and possible contaminants that are produced during bombardment are $^{55,57,58,61}Co$ and $^{60,61,62}Cu$.

To identify the possible impurities from the final product, the radionuclide purity were assessed by using gamma-ray spectrometry method. The radionuclide purity of $^{64}CuCl_2$ solution was assessed using the HPGe detector located at CCR. The optimum distance between the

sample and the detector was selected according to sample activity so that the dead time is less than 10%.

The gamma spectrum acquired before purification step is presented in Figure 4, where the expected cobalt isotopes ^{56}Co, ^{57}Co, ^{58}Co, were identified.

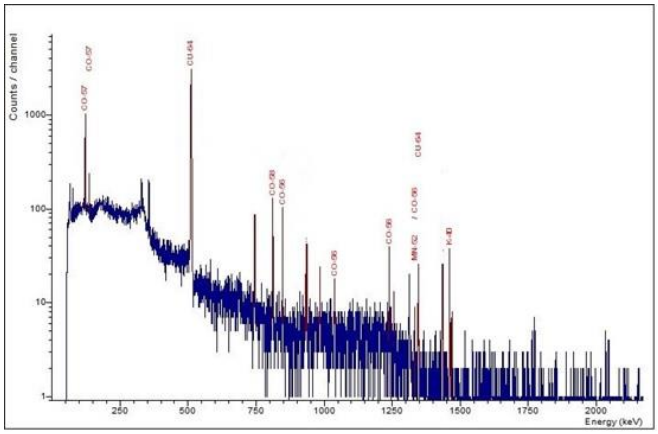

Figure 3. Gamma spectrum acquired before purification

As expected, the radionuclides with short half-lives, such as ^{60}Cu, ^{61}Cu and ^{62}Cu, were not detected in the analyzed sample, the sample being measured at 24 h after EOB. The radionuclide purity was calculated to be 92.65 %. After purification, a sample consisting in 2 µl of $^{64}CuCl_2$ was analyzed, identifying the characteristic peaks of ^{64}Cu and checking the presence of other possible radionuclide impurities.

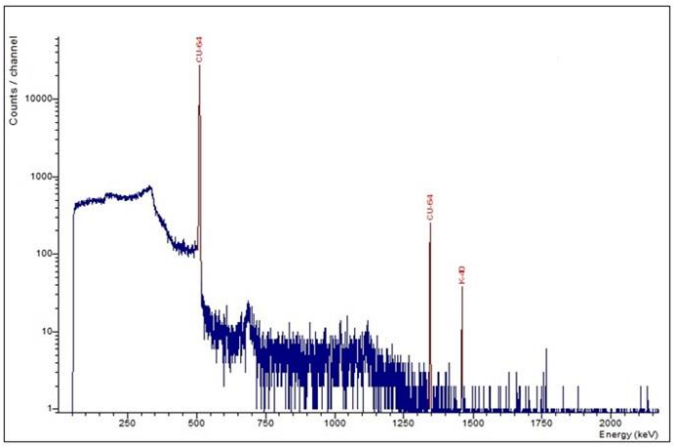

Figure 4. Gamma spectrum acquired after purification, acquisition time of 30 minutes. The gamma lines corresponding to ^{64}Cu isotope are marked on the figure.

The gamma spectrum presented in Figure 5 shows that only the characteristic peak of ^{64}Cu (1345 keV) and the annihilation peaks (511 keV) were identified, confirming the high yield of separation and the excellent radionuclide purity > 99.99% of purified $^{64}CuCl_2$ solution.

The same sample of 2 μl of $^{64}CuCl_2$ was analyzed for an acquisition time of 12 h to double check the presence of possible radionuclides contaminants.

It was observed that in the spectrum acquired for a longer acquisition time there are no other contaminants, being identified only the radionuclide of interest ^{64}Cu. The other peaks identified in the spectrum come from the natural background of radiation.

Another quality test of the final solution is the radionuclide identity by measuring the half-life. The measured half-life of the final solution was determined by successive counting of activity by using the dose calibrator.

The measured value of the half-life was 12.43 h, 2.1% under the reference value of 12.7 h, being in the ± 5% accepted range.

4.2.2 The use of the ^{64}Cu solution as a radiotracer for PET/CT imaging

The assessment of the quality for the ^{64}Cu radionuclide produced by using 99.53% enriched ^{64}Ni, TR-19 Cyclotron and the automated solid target system, reaching a total activity greater than 200 mCi was performed for further investigation by PET imaging.

The PET/CT scans for one mouse bearing a prostate cancer cell (DU-145) injected with $^{64}CuCl_2$ as tracer were performed using the MicroPET system from MILabs installed at CCR, IFIN-HH.

4.2.2.1 Animal preparation and acquisition

The MicroPET system has two beds, one for mouse and the other one for rat, similar in terms of mounting mechanics and the main difference lies in the field of view. In the case discussed in this thesis, the mouse bed was used. The fitting of the animal in the bed has to be completely because any parts extending beyond the contours of the animal bed can collide with the collimator and therefore disturb the measurements, resulting in artefacts in the reconstructed PET images.

The essential parameters such as frames (number of time frames and time per frame), scan mode (multi-planar, spiral) step mode (fine, normal, fast) and acquisition mode (list-mode, isotope) were set prior to perform the scans in the PET-CT modes.

The preparation of CT consists in terms of CT calibration and heating, taking into account that the X-ray source needs a warm-up time when it has not been used for more than 2 hours.

Once the animal to be scanned is fixed in the position and the scan parameters presented above are set, the acquisition is started.

The mouse bearing a prostate cancer (DU-145) was scanned for around 40 minutes, immediately after injection and 2 hours after injection. The mouse was injected with 11.3 MBq $^{64}CuCl_2$.

4.2.2.2 Reconstruction of the acquired data

For the reconstruction of the acquired data the MILabs-Rec provided software was used. The software allows automatic data transfer from the acquisition computer to the reconstruction computer. To transfer the data is required that both of the acquisition computer and the reconstruction one to be operating and connected between.

To obtain the higher details in the reconstructed image, the voxel size has to be as small as possible (for example 0.2 mm), but also the time to perform the reconstruction it will be longer. The steps to be followed to create a reconstructed image consist in data selection, PET/CT reconstruction, processing of the data and quantified PET/CT image.

The choice of the number of subsets and iteration is linked to the amount of acquired counts: for low counts are chosen 4 subsets, for medium counts are chosen 16 subsets, while for high counts it is recommended to choose 32 subsets. By choosing a large number of iterations it is obtained a good resolution, but the noise is higher in the reconstructed image. For the optimal choice of the number of iterations, both the resolution and the resulting noise must be considered. The best compromise for getting the best results for both of them has to be found.

4.2.2.3 Image processing of the reconstructed data

The image processing of the reconstructed data was performed by using the PMOD software [25] useful to load images in different formats, to view the images using various color, to perform different image processing and display fusion images (from PET/CT) of the matched data sets.

Figure 5 are presented the CT scan, PET scan and PET/CT fusion for the mouse bearing a DU-145 tumor, injected with 11.3 MBq of $^{64}CuCl_2$, scanned immediately after injection. It was observed that the radioactive solution is present only at the injection site, which was the tail and the eye.

Figure 6 presents the PET/CT fusion for the same mouse, scanned at 2 h after injection time.

From Figure 6 it can be seen that at 2 hours post injection the radioactive solution migrated from the injection site to the organs such as kidneys, liver, stomach, bladder. This was also observed from the values of activities after biodistribution measured by using a dose calibrator.

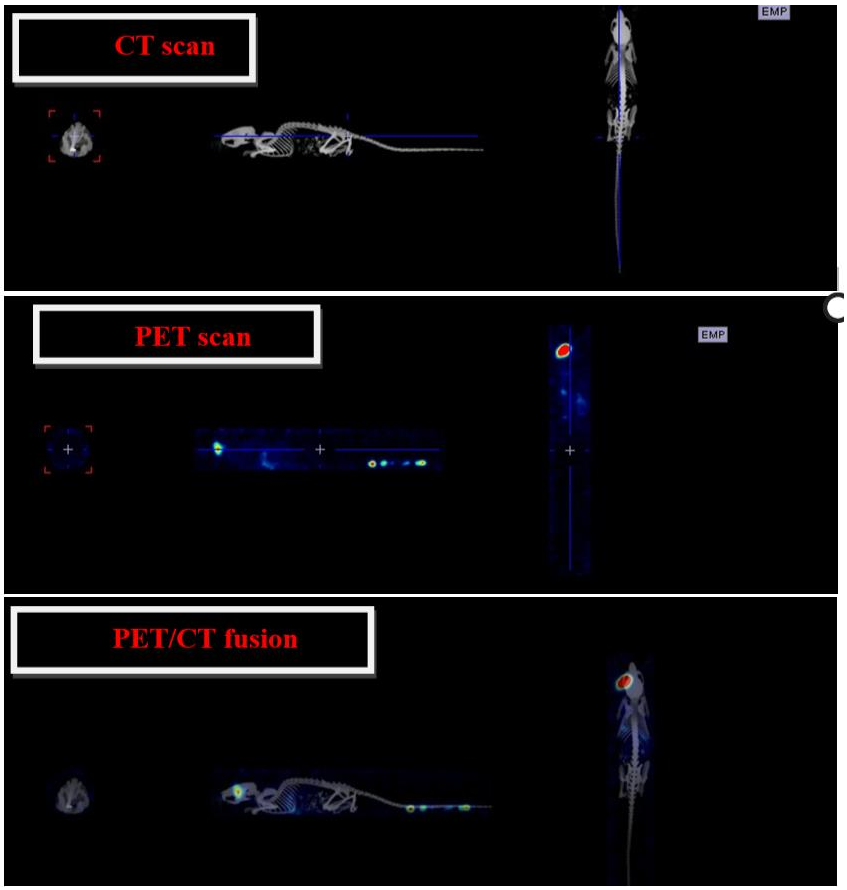

Figure 5. PET/CT images for the mouse bearing a DU-145 tumor, scanned immediately after injection.

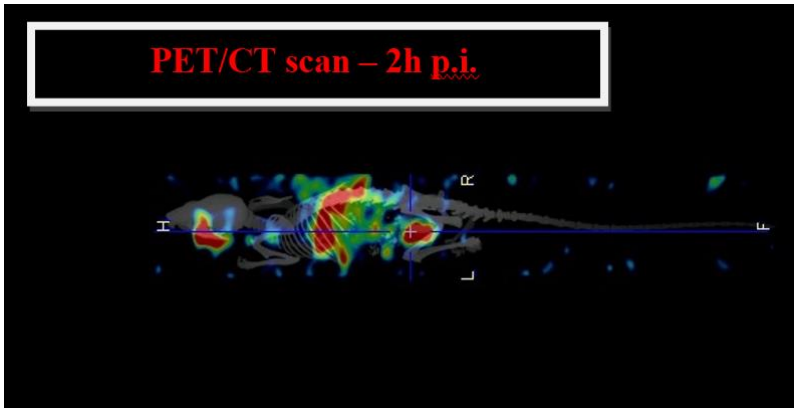

Figure 6. PET/CT image for the mouse bearing a DU-145 tumor, scanned at 2 h post injection.

5 Monte Carlo simulations for production of medical radioisotopes by using photonuclear reactions with gamma beams at ELI-NP facility

In the present time, these radioisotopes are produced in the vast majority of the cases through reactions nuclear involving nuclear reactors or by using charged particles by using cyclotrons or other types of linear accelerators.

An example was already presented in Section 5.2., where ^{64}Cu radioisotope, with relatively long half-life, was produced by the most used method, namely by using enriched ^{64}Ni targets via (p,n) nuclear reaction.

The other option to produce radioisotopes can be the gamma beams which are exciting neutron or proton into an unbound state causing to photo-dissociation resulting in this way a new isotope.

For example, the radioisotope ^{64}Cu can be produced by photonuclear reaction (γ, n) using ^{65}Cu as the irradiation target.

The ELI-NP VEGA system will deliver an intense photon beam with specifications in terms of photon flux, brilliance and energy bandwidth with maximum photon energy of 19.5 MeV all these parameters being suitable for radioisotopes production.

The VEGA system is based on inverse-Compton scattering (ICS), where gamma ray photons are generated by backscattering of laser photons off a relativistic electron beam.

All the parameters that will become available for the gamma beams at ELI-NP are suitable for radioisotopes production, which is why Monte Carlo simulations to obtain ^{64}Cu and ^{99}Mo radioisotopes using photonuclear reactions (γ, n) have been performed [26].

With these considerations, we investigated the possibility of producing radioisotopes of medical interest through Monte Carlo simulation of photo-neutron reactions using the high-intensity gamma beams.

5.1 Production of the gamma beams through Inverse Compton Scattering at Extreme Light Infrastructure – Nuclear Physics, ELI-NP

The name of Inverse Compton Scattering comes from the fact that through this process photons are the ones that acquire energy as compared to the classical Compton effect in which electrons acquire energy.

In the Inverse Compton Scattering process, the energy of the scattered photons depends on the energy of the electron beam, the energy of the laser photons, the laser incident angle, and the scattering polar angle of the scattered photons with respect to the electron direction of propagation

The energy range for the produced gamma-rays at ELI-NP is from 1 MeV to 19.5 MeV, with the energy of the electron beam from 250 to 750 MeV.

The energy of the scattered gamma-rays as a function of the electron beam energy is shown in Figure 7.

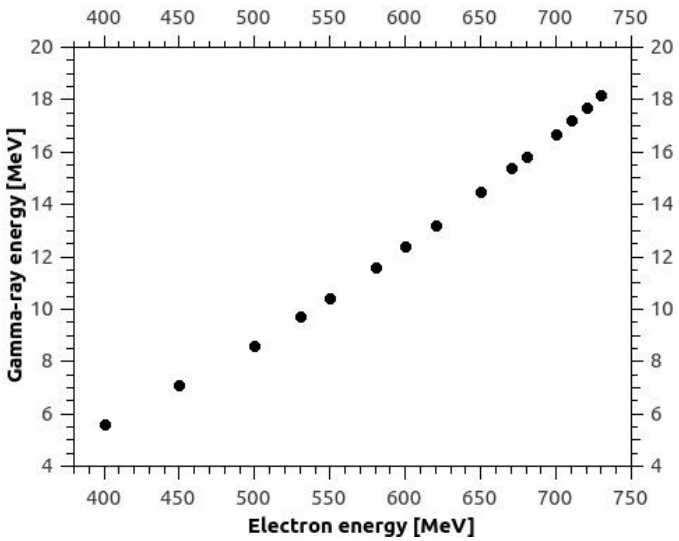

Figure 7. The energy of the scattered gamma-rays as a function of the electron beam energy.

In this context it was investigated the production possibility of medical radioisotopes such as ^{64}Cu and ^{99}Mo by using photo-nuclear reactions with ELI-NP gamma-ray beam by Monte Carlo simulation.

5.2 $^{65}Cu(\gamma,n)^{64}Cu$ Case

The study case of ^{64}Cu radioisotope production via (γ,n) photonuclear reaction on ^{65}Cu targets was selected to compare the results of the activities obtained by using both proton induced nuclear reaction and photonuclear reactions.

An outcome of this comparative study consists in highlighting the advantages and disadvantages of the two types of reactions in the production of radioisotopes for medical treatment.

One of the advantages is related to the target materials used for the two types of reactions. As compared to ^{64}Ni (for the proton induced reaction) with a very low natural abundance of 0.93%, ^{65}Cu (for the photonuclear reaction) has a relatively high natural abundance of 30.85% and the resulting production route further saves the chemical separation step.

To model the radioisotopes production using gamma-ray beams, the gamma beam simulation code [27] was combined with GEANT4 toolkit [28] to model the gamma beam production and to study the spectral and flux density distributions of the gamma beam during its transport from the laser-electron interaction point to the target.

The combined code included the geometry of a thin isotopic target with flexible radius placed in front of the beam for the generation of radioisotopes of interest.

Similar to the activity calculation when using the (p,n) nuclear reaction, the photo-nuclear reaction yield has to be calculated and then the specific activity of ^{64}Cu medical radioisotope by using (γ,n) photonuclear reaction can be extracted.

To obtain the specific activity of the ^{64}Cu radioisotope, a cylindrical target of ^{65}Cu with density of 8.96 g/cm^3 and a total gamma-beam flux of 10^{11} γ/s (corresponding to a collimated gamma beam flux of about 10^9 γ/s) was employed in the simulation.

The other input parameters used in the simulation were the target thickness of 1 cm and a radius of 2 mm and the irradiation time of 80 h.

Figure 8 shows the specific activity of ^{64}Cu radioisotope produced by photo-neutron reactions as a function of incident gamma-ray energies, where the irradiation time was 80 hours.

It was found based on the simulations that for given isotopic target dimension, the end-point energy of 17.2 MeV, corresponding to the 710 MeV electron-beam energy, the highest specific activity of ^{64}Cu was obtained.

By selecting different electron beam energies to obtain the end-point energy of the gamma rays, the specific activity of ^{64}Cu as a function of the target thickness was calculated and plotted in Figure 9.

From Figure 9 one can be observed that the thinner the isotopic target, the higher specific activity was obtained, the specific activity decreasing rapidly with the increasing of the target thickness. It was showed that the highest specific activity of 1.2 mCi/g can be achieved considering a thin target with radius of 2.0 mm and thickness 1.0 cm.

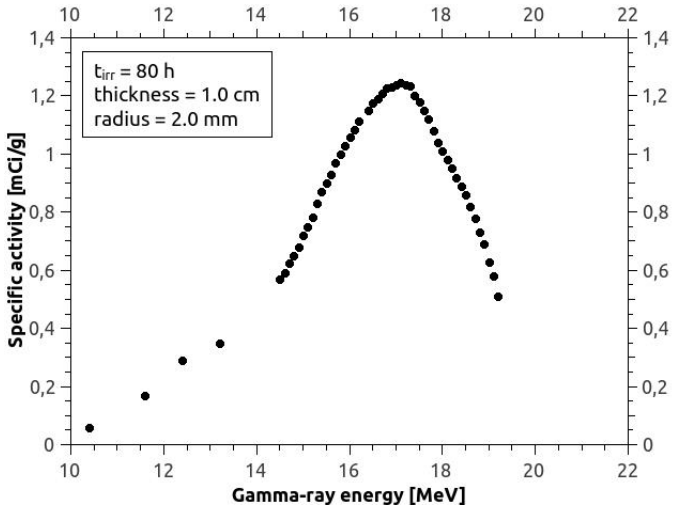

Figure 8. Specific activity of ^{64}Cu radioisotope as a function of the incident γ-rays energy for given target geometry and irradiation time.

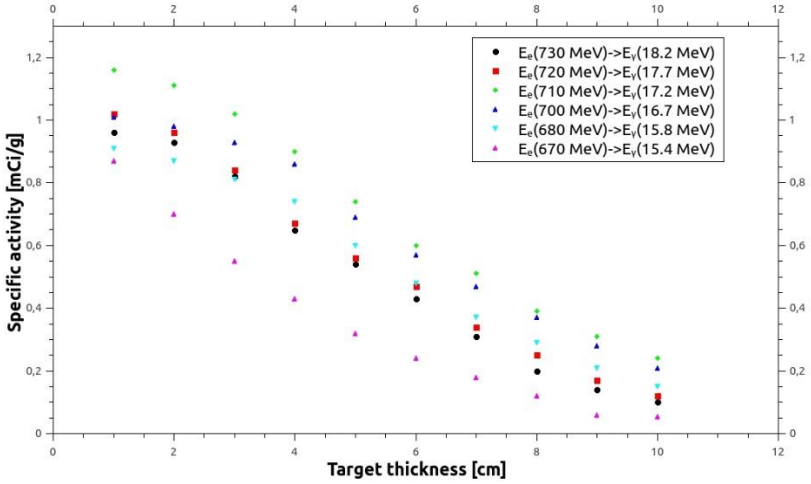

Figure 9. Specific activity of ^{64}Cu radioisotope as a function of the target thickness; Target radius of 2 mm. The data are plotted for different electron beam energies used in the generation of gamma beams.

Different values of the irradiation time were also employed in the simulation to obtain the saturation activity. It was observed that by using an optimal energy of the gamma beam (17.2 MeV) and a small thin target (radius 2.0 mm and thickness 1.0 cm), the specific activity of the ^{64}Cu radioisotope reaches 0.88 mCi/g after one day irradiation, while the specific activity has a saturation value exceeding 1.2 mCi/g that can be reached after irradiation times of the order of 5-6 times the radioisotope half-life (about 80 h).

In a similar manner simulations of the ^{65}Cu(γ,n)^{64}Cu reactions were performed with a different isotopic target, in order to determine whether the maximum specific activity can be improved. The ^{65}Cu target was replaced in the simulations with a ^{65}CuO target to obtain ^{64}Cu

radioisotope. In the simulation, we considered the oxide ^{65}CuO target as the irradiation target with a density of 6.31 g/cm^3.

By comparing the results obtained when irradiating ^{65}CuO target with the previous results from the irradiation of the ^{65}Cu it appears that using ^{65}Cu target is more advantageous, the difference between the obtained specific activities being of about 17%.

Based on the simulations performed for ^{64}Cu radioisotope production via photo-neutron reactions one can conclude that due to the very low specific activities that can be achieved, these photo-nuclear reactions are not suitable for generating the radioisotope for use as radiopharmaceutical.

5.3 $^{100}Mo(\gamma,n)^{99}Mo$ Case

The study of $^{99}Mo/^{99m}Tc$ production via photo-nuclear reactions was selected because the cross section for the $^{100}Mo(\gamma,n)$ reaction is very well-known and its separation processes and the associated technology are well-defined. Production of this radioisotope via photo-nuclear reaction (γ,n) was considered of high interest for the possible applications that can be developed at ELI-NP.

Presently, the most spread method worldwide to produce $^{99}Mo/^{99m}Tc$ is via neutron induced reactions in nuclear reactors. One of the alternative methods considered to produce $^{99}Mo/^{99m}Tc$ is by using (γ,n) photo-nuclear reaction involving ^{100}Mo targets.

In order to estimate the specific activity of $^{99}Mo/^{99m}Tc$ using gamma beams similar simulations with the case of ^{64}Cu production were performed.

To obtain the specific activity of $^{99}Mo/^{99m}Tc$, in the simulation the oxide $^{100}MoO_3$ was considered as irradiation target with a density of 4.7 g/cm^3.

Figure 10 shows the specific activity of $^{99}Mo/^{99m}Tc$ radioisotopes produced by photo-nuclear reactions as a function of incident γ-rays energy where the irradiation time was 100 hours. The $^{100}MoO_3$ target with radius of 2.0 mm and thickness of 1.0 cm was used.

The results presented in Figure 10 confirm that the highest value of the activity was for the gamma beam end-point energy of 14.5 MeV corresponding to the 650 MeV electron beam energy.

In the simulations the isotopic target dimension was also optimized, at defined irradiation time interval (100 h) such to maximize the activity of the radioisotope.

Figure 11 presents the simulated activities of the $^{99}Mo/^{99m}Tc$ as a function of the target thickness, while the radius of the target was kept fixed of 2 mm.

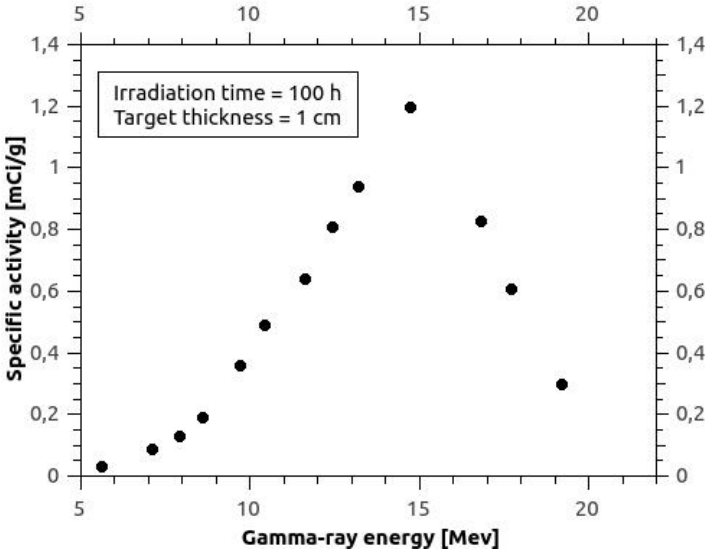

Figure 10. Specific activity of ^{99}Mo/^{99m}Tc radioisotope as a function of the incident γ-rays energy following the irradiation for 100 hours of a 1 cm thick target.

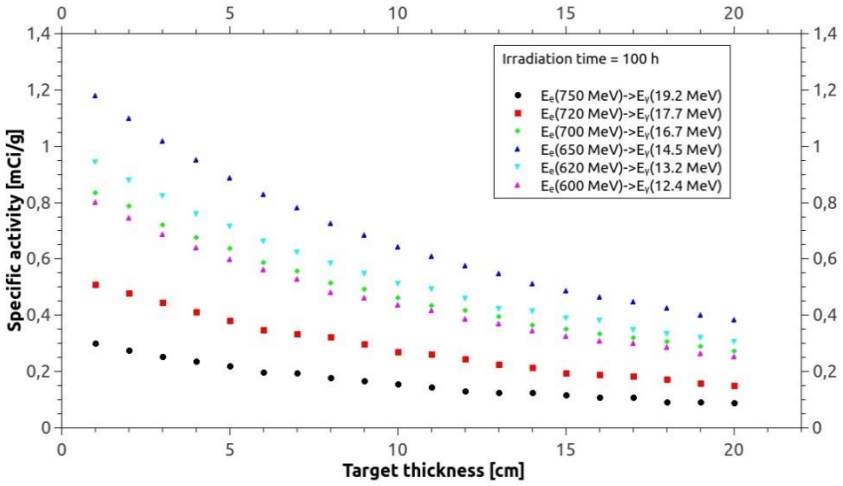

Figure 11. Specific activity of ^{99}Mo/^{99m}Tc as a function of the target thickness at different electron beam energies. The considered irradiation time is of 100 hours and the target radius is 2 mm.

The activity obtained for the optimal gamma-ray energy of 14.5 MeV was 1.2 mCi/g by using as input parameters a thin target with radius of 2 mm and thickness of 1 cm.

It was also observed that using an optimal γ-beam energy (14.5 MeV) and a thin target (radius 2 mm and thickness 1 cm), the specific activity of the ^{99}Mo radioisotope reached 0.56 mCi/g after one day irradiation, while the specific activity has a saturation value exceeding 1.2 mCi/g after 100 h irradiation and 2.4 mCi/g after about 5-6 times half-life irradiation time (around 300 h).

Also, in the case of $^{99}Mo/^{99m}Tc$ generators for nuclear medicine, based on the predicted specific activities, the production via photo-nuclear reactions does not seem to be attractive for practical purposes.

6 Results and discussions regarding ^{64}Cu radioisotope production

6.1 Photonuclear reactions activity results vs nuclear reactions activity results for ^{64}Cu radioisotope

Simulations for production of ^{64}Cu radioisotope of medical interest through photo-nuclear reactions using the high-intensity quasi-monochromatic gamma-beam of the Extreme Light Infrastructure – Nuclear Physics (ELI-NP) facility were presented.

Simulations of the inverse Compton scattering process were performed by modifying the electron-beam energy to obtain gamma-ray beams of different energies and then the optimal energy to produce ^{64}Cu radioisotope was identified.

The optimal energy for the production of the radioisotope of interest was chosen in accordance with the maximum values of the reaction cross sections from existing databases, thus maximizing the calculated specific activity for the ^{64}Cu radioisotope.

The specific activity of ^{64}Cu by using the $^{65}Cu(\gamma,n)$ reaction was calculated as a function of target geometry, irradiation time and gamma-beam energy.

As an alternative method, the specific activity of ^{64}Cu by using oxide targets of ^{65}CuO was calculated as a function of target geometry, irradiation time and gamma-beam energy to observe the difference when using different types of irradiation targets. The obtained results of the specific activity were better with the metallic target of ^{65}Cu, with a specific activity higher with 17% as compared to the oxide target.

Using the Monte Carlo simulations, we estimated that after irradiation times of the order of 5–6 times the half-life, a specific activity of the order of 1.2 mCi/g can be achieved for a thin target (radius 1–2 mm, thickness 1 cm), considering a total gamma beam flux of 10^{11} photons/s.

To obtain the saturation specific activity, the irradiation time was varied in the calculations from 1 h to 80 h.

Considering the possibility of producing ^{64}Cu radioisotopes, as well as other radioisotopes of interest for nuclear medicine, it can be concluded that, as compared to the current methods of radioisotope production, a gamma beam facility would generate almost no nuclear waste, and that, by using the high-intensity quasi-monochromatic gamma beam from ELI-NP, photo-nuclear reactions can be viewed as a new production route for radioisotopes production for radioisotopes of medical interest.

In a similar way, simulations were performed to produce the ^{64}Cu radioisotope in cyclotron using the ^{64}Ni (p, n) nuclear reaction. In this case also experimental measurements to validate the simulations were performed.

The simulations performed aimed to optimize the irradiation parameters such as proton beam energy, irradiation time and current to obtain a maximum production yield.

The simulations were verified by performing an experiment in which the same irradiation parameters involved in the simulations were used. The difference between the activity obtained from the experiment and that resulting from the simulation was 14%, being expected and considered acceptable due to the purification process, geometry and uneven distribution of the target resulting during the electrodeposition process.

The use of both ^{64}Cu radioisotope production methods - by (γ,n) photo-nuclear reaction and by (p,n) nuclear reaction - allowed for the comparison of the specific activities and to highlight the advantages and disadvantages of using one or the other of the two production routes.

By using the ^{65}Cu(γ,n)^{64}Cu photo-nuclear reaction a specific activity of 1.22 mCi/g was obtained, while using the ^{64}Ni(p,n)^{64}Cu nuclear reaction a carrier free ^{64}Cu is obtained, with the simulated activity of 5.84 mCi/g and the experimental obtained activity of 236 mCi/0.0474 g =4.98 mCi/g.

7 Conclusions

The present work aimed at studying the possibility of producing ^{64}Cu radioisotope, optimizing the irradiation parameters in order to maximize the reaction yield and implicitly the specific activity.

The ^{64}Cu radioisotope is important for use as a radiopharmaceutical, given that it is among the only known radionuclides in nuclear medicine that presents the three modes of decay, namely positron decay, beta minus decay, and electron capture. This physical characteristic of the decay of the ^{64}Cu radionuclide leading to positron emission and emission of beta particles and Auger electrons and, together with the relatively short half-life of 12.7 h make it suitable for use both for diagnostic purposes and in the therapeutic ones, being thus called the teranostic radioisotope.

Previous studies have shown that ^{64}Cu can be produced using nuclear reactors [87], or using proton irradiated targets to cyclotron [69], resulting in greater accessibility to this radioisotope. The choice to produce ^{64}Cu at the reactor leads to high or low specific activity values depending on the chosen method, by direct activation (n,γ) or indirectly through (n,p) reaction on a Zn targets.

The methods that are feasible for nuclear medicine application have been developed only relatively recently, indicating that the highest specific activity is achieved by cyclotron irradiation enriched ^{64}Ni targets [68].

Considering all these aspects, the first chapters of the work, 1 – 3, presented the basic theoretical and experimental aspects of the subject, as described in literature, while the original work is presented in the chapters 4 – 6, where the possibility of ^{64}Cu radioisotope production was investigated.

The first step in this study was to estimate the ^{64}Cu radioisotope production via the (p,n) nuclear reaction by using ^{64}Ni enriched targets. For this purpose, simulations were performed in GEANT4 by modelling the solid target used in the experiments and the parameters of the nuclear reaction induced by the protons. To maximize the reaction yield, various irradiation parameters were varied, such as irradiation current and irradiation time.

Taking into account that the energy range of the protons accelerated by the TR-19 cyclotron of IFIN-HH is between 14 - 19 MeV, a 320 μm thick aluminum foil was used to degrade the protons energy from 14 MeV to an average value of 11.7 MeV, the energy corresponding to the maximum value of the reaction cross section, and thus, leading to a maximum reaction yield.

In the simulations two types of ^{64}Ni targets with different degrees of enrichment were used as this is relevant from the involved costs point of view.

The calculated activities obtained by varying the ^{64}Ni targets' degree of enrichment showed an increase of only 3% when going from 95% to 99.53% enrichment. It was shown that by using a ^{64}Ni target enriched to 99.53% a value of 10.3 GBq activity was obtained as compared to 9.3 GBq obtained when using a ^{64}Ni target enriched to 95%.

The second step consisted in performing a real experiment designed to produce the ^{64}Cu radioisotope at the TR-19 cyclotron of IFIN-HH by using the same conditions for the (p, n) nuclear reaction as the ones included in the simulations performed at the first step, namely: t_{irr} = 4h, I = 20 μA, E_p = 14 MeV degraded to 11.7 MeV by using 320 μm aluminum foil. The experiment was conceived such as to allow for a comparison between the results from the experiment and simulation works, and thus, to validate the simulation code.

The determination of the ^{64}Cu radionuclide's purity and half-life was performed by using a $^{64}CuCl_2$ solution. The gamma-ray activity of the sample was performed with a HPGe detector with 25% relative efficiency, placed in Spectrometry Laboratory from Radiopharmaceutical Research Center (CCR) and a radionuclide purity higher than 99.99% was determined. The quality of the produced samples was also validated by the measured half-life of 12.43 hours, a value that is 2.1% under the reference value of 12.7 h, and thus, within the ± 5% accepted range.

A further assessment of the quality of the ^{64}Cu sample produced by using 99.53% enriched ^{64}Ni isotope, with a total activity larger than 200 mCi, was performed by PET imaging, as discussed in Section 4.2.2 and it was observed that in the case of the mouse scanned immediately after injection the radioactive solution is present only at the injection site, while at 2 hours post injection the radioactive solution migrated from the injection site to the organs such as kidneys, liver, stomach, bladder.

Monte Carlo simulation of the ^{64}Cu radioisotope production route is in good agreement with the experimental results obtained through ^{64}Ni(p,n)^{64}Cu reaction, at TR-19 cyclotron. By comparing the activity of ^{64}Cu produced experimentally versus the simulated activity a 14% difference was observed. This is a very good result, as the real production process includes effects that are not included in the simulation, such as process losses during target irradiation and transfer, uncertainties in the activity measurements and cross-section values, target assemble

geometry and mass distribution of the target, unavoidable activity loss in the post-irradiation processing (dissolution and purification).

In conclusion, the simulation code was validated by the experimental results and one can consider this code as providing realistic estimates for the production of radionuclides following (p,n) nuclear reactions at the TR-19 cyclotron. The confirmation of the simulated results with such a narrow error gives confidence to use this simulation code for the optimization of production processes aimed for pharmaceutical grade radioisotopes of medical interest, with different energy ranges, on the same configuration of the automated solid target system, e.g. $^{89}Y(p,n)^{89}Zr$, $^{68}Zn(p,n)^{68}Ga$, $^{44}Ca(p,n)^{44}Sc$.

In the present work the possibility of radioisotopes production by using photonuclear reactions with intense quasi-monochromatic gamma beams was also studied. This study was triggered by the availability in the near future of a high-intensity quasi-monochromatic gamma beam system (VEGA System) at the Extreme Light Infrastructure – Nuclear Physics (ELI-NP). The VEGA System presents all the needed characteristics to investigate and optimize the production of radioisotopes for medical applications.

The production of two radioisotopes of medical interest was investigated via (γ,n) photonuclear reactions.

The first case studied was that of the ^{64}Cu radioisotope produced by (γ,n) reaction on ^{65}Cu target. Production of ^{64}Cu radioisotope via photonuclear reactions was chosen as a mean to compare the results of the activities obtained by using both nuclear reactions (p,n) at cyclotron and photonuclear (γ,n) reaction at ELI -NP. This comparison was used to highlight the advantages and disadvantages of the two types of reactions in the process of producing the radioisotope of medical interest ^{64}Cu, as well as to identify effective ways to improve/optimize the production conditions. The optimal value of the gamma beams energies used in the simulations to maximize the reaction yields and implicitly of the specific activities were chosen according to the maximum values of the measured reaction cross-sections from EXFOR databases. In the case of ^{64}Cu production via the $^{65}Cu(\gamma,n)^{64}Cu$ reaction, the optimal energy value of the gamma-ray beam is 17.2 MeV where the maximum value of the cross section from the EXFOR database is 90.1 mb. The specific activity of ^{64}Cu by using the $^{65}Cu(\gamma,n)$ reaction was calculated as a function of target geometry, irradiation time and gamma-beam energy. The obtained results showed that after 5–6 times the half-life irradiation time, a specific activity of about 1.2 mCi/g can be achieved for a thin target (radius 1–2 mm, thickness 1 cm). Similar to simulations performed for $^{65}Cu(\gamma,n)^{64}Cu$, it was also interesting to change the chemical composition of the target, in order to observe if the maximum specific activity can be improved. It was shown that when using a ^{65}CuO oxide target a lower specific activity by about 17% was obtained as compared to the case of ^{65}Cu target.

The very low specific activity of 1.2 mCi/g predicted in the simulation by using the $^{65}Cu(\gamma,n)^{64}Cu$ photonuclear reaction shows that the flux of the gamma beams has to be increased by two order of magnitude to obtain comparable specific activities to the (p,n) reaction.

The disadvantage of using the (p,n) nuclear reaction at cyclotron, using enriched Ni targets is that the targets are more expensive, as compared to the use of photonuclear reactions on ^{65}Cu targets with a natural abundance.

The second case of photonuclear reaction considered in simulations was that of ^{99}Mo/^{99m}Tc production. The reason to study this case is justified by its well-recognized importance for the cancer therapy, by the good knowledge of the cross section for the ^{100}Mo(γ,n) reaction and of its separation processes and the associated technology. In this case the maximum cross section for the (γ,n) reaction on ^{100}Mo is 150 mb corresponding to an incident γ-ray energy of Eγ = 14.5 MeV. By considering a thin target of radius 2 mm and thickness 1 cm of oxide $^{100}MoO_3$ a specific activity of the ^{99}Mo radioisotope of 0.56 mCi/g was computed after one day irradiation, while the saturation specific activity has a value of 2.4 mCi/g and it is achieved after about 5-6 times half-life irradiation time (around 300 h).

Similarly to the case of ^{64}Cu, the predicted specific activity of ^{99}Mo for production of ^{99}Mo/^{99m}Tc generators for nuclear medicine is too low for real practical purposes.

In the future, the optimization of irradiation parameters for the photonuclear reactions is considered to obtain specific activities similar to those obtained by using charged particles and to make photonuclear reactions suitable to produce radioisotopes for nuclear medicine. At the VEGA System of ELI-NP one can use the simulation code discussed in the thesis to optimize different production schemes and to validate them experimentally and to propose the production at future more intense gamma beam systems.

The results of the research presented in this thesis have been published in scientific articles in journals indexed in the ISI-Clarivate Analytics system and / or communicated at international conferences, as follows:

1. *Determination of the ^{60}Co source activity by using the sum-peak method*, **S. Ilie**, C. A. Ur, O. Sima, G. Suliman, A. Pappalardo, Romanian Reports in Physics, Vol. 71, No 4, 211, 2019;
2. *Unfolding of sparse high-energy γ-ray spectra from LaBr3:Ce detectors*, Capponi, V. Iancu, D. Lattuada, A. Pappalardo, G.V.Turturică, E. Açıksöz, D.L.Balabanski, P.Constantin, G.L. Guardo, M. Ilie, S. Ilie, C. Matei, D. Nichita, T. Petruse, A. Spataru, Journal of Instrumentation, Volume 14, November 2019
3. *Process validation for production of copper radioisotopes in a TR-19 variable energy cyclotron*, R. A. Leonte, D. Cocioabă, L. E. Chilug, **S. I. Băruță (Ilie)**, T. R. Eșanu, B. Burghelea, A. Chiriacescu, L. S. Crăciun, and D. Niculae, Harnessing Isotopes for Improved Quality of Life AIP Conf. Proc. 2295, 020022-1–020022-7, 2019;
4. *Characterization of the segmented high-purity germanium clover detector from the ELIADE array at ELI-NP*, **Simona Băruță (Ilie)**, Călin A. Ur, Octavian Sima, Gabriel Suliman, Gabriel V. Turturică, Violeta Iancu, U.P.B. Sci. Bull., Series A, Vol. 83, Iss. 2, 2021;
5. *Systematic influences on the areas of peaks in gamma-ray spectra that have a large statistical uncertainty*, M. Bruggeman, S.M. Collins, L. Done,M.Durasevic, M.A. Duch ,A. Gudelis, M.Hyza, A. Jevremovi, A. Kandi ,M. Korun, **S. Ilie**, J.M. Lee, K.B. Lee, A. Luca, R.M. Margineanu, A. Pantelica, I. Serrano, B. Seslak, L.C. Tugulan, L. Verheyen, B. Vodenik, I. Vukanac, Z. Zeng, B. Zorko, Applied Radiation and Isotopes (2017);
6. *High-resolution gamma-ray spectroscopy with eliade at the Extreme Light Infrastructure*, P.-A. Söderström, G. Suliman, C.A. Ur, D. Balabanski, T. Beck, L. Capponi, A. Dhal, V. Iancu, **S. Ilie**, M. Iovea, A. Kusoglu;C. Petcu, N. Pietralla, G.V. Turturica, E. Udup, J. Wilhelmy, A. Zilges, Acta Physica Polonica B, Vol. 50, No. 3, (2019);
7. *Forecasting the production of medical radioisotopes at Extreme Light Infrastructure - Nuclear Physics gamma beam system*, D. Niculae, F. D. Puicea, **S. Ilie**, W. Luo, P. V. Cuong, G. Cata Danil, C. A. Ur, D. Balabanski, Eur J Nucl Med Mol Imaging (2017) 44 (Suppl 2):S119–S956, 2017;
8. *Production of Copper Medical Radioisotopes in a Variable Energy Cyclotron*, Dana Niculae, Radu Leonte, Livia Chilug, Ramona Dusman, **Simona Baruta**, Diana Cocioaba, Liviu Craciun, NUSPRASEN Workshop on Nuclear Science Applications, Helsinki, Finland, November 25-27, 2019;
9. *High energy gamma beam forecasted for production of new and emerging medical radioisotopes by photonuclear reactions, 13th International Symposium on the Synthesis and Applications of Isotopes and Isotopically Labelled Compounds*, Dana Niculae,

Simona I. ILIE , Livia Chilug, Filip D. Puicea, Calin A. Ur , Dimiter L. Balabanski Czech Republic, Prague, June, 3-7, 2018, (Poster);

10. *Assessment of radioisotopes production for medical applications at ELI-NP*, **Simona Ilie**, Dana Niculae, C. A. Ur, 17th International Balkan Workshop on Applied Physics and Materials Science (IBWAP 2017), Constanta, Romania, July 11-14, 2017, Oral Presentation;
11. *Development of new production routes, separation and purification methods of ^{99}Mo and ^{99m}Tc, New 2nd CRP Meeting on Ways of Producing Tc-99m and Tc-99m Generators (Beyond fission and cyclotron methods)*, Dana Niculae, D. Balabanski, C.A. Ur, **Simona Baruta**, Warsaw, Poland, May 13-17, 2019
12. *Characterisation of the segmented clover detectors from the ELIADE array at ELI-NP"*, **Simona Ilie,** Sixth International Conference on Radiation and Applications in Various Fields of Research, RAD 2018, June 17-26, 2018, Oral Presentation
13. *Determination of the ^{60}Co source activity by using the sum-peak method"*, **Simona Ilie,** Seventh International Conference on Radiation and Applications in Various Fields of Research, RAD 2019, June 09 – 15, 2019, Oral Presentation

8 References

1. B. R. Martin, Nuclear and Particle Physics, John Wiley & Sons, Ltd., 2006, p. 415.
2. H. Becquerel, "Sur les radiations émises par phosphorescence," *Comptes Rendus,* pp. 420-421, 1896.
3. J. J. Thomson, "Cathode Rays," in *Proceedings of the Royal Institution of Great Britain*, 1897.
4. P. Radvanyi and J. Villain, "The discovery of radioactivity," *Comptes Rendus Physique,* vol. 18, no. 9-10, pp. 544-550, 2017.
5. H. Günther and V. Müller, Einstein ’s Energy–Mass Equivalence, Springer, Singapore, 2019.
6. H. Hettema, "Bohr's theory of the atom 1913–1923: A case study in the progress of scientific research programmes," *Studies in History and Philosophy of Science Part B: Studies in History and Philosophy of Modern Physics,* vol. 26, pp. 307-323, 1995.
7. V. Nesvizhevsky and J. Villain, "The discovery of the neutron and its consequences (1930–1940)," *Comptes Rendus Physique,* vol. 18, pp. 592-600, 2017.
8. E. G. Segrè, "The Discovery of Nuclear Fission," *Nuclear Fission. Physics Today,* vol. 42, no. 7, pp. 38-43, 1989.
9. E. O. Lawrence, "Method and apparatus for the acceleration of ions, filed:". Patent U.S. Patent 1,948,384, 26 January 1932.
10. T. H. Maiman, "RUBY LASER SYSTEMS". 14 November 1967.
11. I. Agarbiceanu, A. Agafitei, L. Blanaru, N. ionescu-Palla, V. Vasiliu and V. Velculescu, in *The Third International Congress on Quantum Electronics*, Paris, 1963.
12. The White Book of ELI Nuclear Physics Bucharest-Magurele.
13. H. Weller, C. Ur, C. Matei, J. Mueller, M. Sikora, G. Suliman, V. Iancu and Z. Yasin, "Gamma beam delivery and diagnostics," *Romanian Reports in Physics,* vol. 68, pp. 447-481, 2016.
14. G. Knoll, Radiation Detection and Measurement, 4th ed., John Wiley & Sons, Inc, 2010.
15. A. Rahmim and H. Zaidi, "PET versus SPECT: strengths, limitations and challenges," *Nuclear Medicine Communications,* vol. 29, no. 3, pp. 193-207, 2008.
16. W.-H. Wong and J. Uribe, "Principles of Single Photon Emission Computed Tomography and Positron Emission Tomography," *Targeted Molecular Imaging in Oncology,* pp. 19-29, 2001.
17. "Recommended data - LNHB," [Online]. Available: http://www.nucleide.org/DDEP_WG/DDEPdata.htm.
18. K. Debertin and R. Helmer, Gamma- and x-ray spectrometry with semiconductor detectors, North-

Holland; Amsterdam (Netherlands), 1988, p. 409.

19. A. J. Tavendale and G. T. Ewan, "A high-resolution lithium-drift germanium gamma-ray spectrometer," *Nuclear Instruments and Methods,* vol. 25, pp. 185-187, 1963.
20. G. Gilmore, Practical Gamma-ray spectrometry, Second ed., John Wiley & Sons, 2008.
21. S. Baruta (Ilie), C. Ur, O. Sima, G. Suliman, G. Turturica and V. Iancu, "Characterisation of the segmented high-purity germanium clover detector from the ELIADE array at ELI-NP," *U.P.B. Sci. Bull., Series A,* vol. 83, no. 2, 2021.
22. A. Luca, B. Neacsu, A. Antohe and M. Sahagia, "Calibration of the high and low resolution gamma-ray spectrometers," *Romanian Reports in Physics,* vol. 64, no. 4, pp. 968-976, 2012.
23. Y. Ogata, H. Miyahara, N. Ishigure, M. Ishihara, M. Nishio and S. Yamamoto, "Development of a modified sum-peak method for activity determination of some gamma emitters," *NuclearInstrumentsandMethodsinPhysicsResearchA,* vol. 775, pp. 34-40, 2015.
24. D. Bazzacco and N. Marginean, "Private Communication, INFN Sezione di Padova, Italy," 1997.
25. S. Ilie, C. A. Ur, O. Sima, G. Suliman and A. Pappalardo, "Determination of the 60Co source activity by using the sum-peak method," *Romanian Reports in Physics,* vol. 71, 2019.
26. B. S. Gopal, Fundamentals of Nuclear Pharmacy, Seventh Edition ed., p. 430.
27. [Online]. Available: http://www.advancedcyclotron.com/cyclotron-solutions/tr19.
28. I. Ursu, L. Craciun, D. Niculae and N. V. Zamfir, "The Radiopharmaceuticals Research Centre of IFIN-HH at Start," *Romanian Journal of Physics,* vol. 58, pp. 1327-1336, 2013.
29. R. A. Leonte, D. Niculae, L. Craciun and G. Cata-Danil, "Medical radioisotopes production at TR-19 cyclotron from IFIN-HH," *UPB Scientific Bulletin Series A: Applied Mathematics and Physics,* pp. 223-236, 2017.
30. B. Mazière, O. Stulzaft, J. M. Verret, D. Comar and A. Syrota, "[55Co]- and [64Cu]DTPA: new radiopharmaceuticals for quantitative tomocisternography," *Int. J. Appl. Radiat. Isot.,* pp. 595-601, 1983.
31. R. A. Leonte, D. Niculae, L. Ș. Crăciun and G. Căta-Danil, "Medical radioisotopes production at TR-19 cyclotron from IFIN-HH," *UPB Scientific Bulletin Series A: Applied Mathematics and Physics,* vol. 79, pp. 223-236, 2017.
32. R. A. Leonte, D. Cocioabă, L. E. Chilug, S. I. Băruță (Ilie), T. R. Eșanu, B. Burghelea, A. Chiriacescu, L. Ș. Crăciun and D. Niculae, "Process Validation for Production of Copper Radioisotopes in a TR-19 Variable Energy Cyclotron," 2020.
33. M. A. Synowiecki, L. R. Perk and J. F. W. Nijsen, "Production of novel diagnostic radionuclides in small medical cyclotrons," *EJNMMI Radiopharmacy and Chemistry,* 2018.
34. K. Maiko, P. Carey, G. Gaehle, E. Madrid, T. Voller, W. Margenau, M. Welch and S. Lapi, "A semi-automated system for the routine production of copper-64," *Applied Radiation and Isotopes,*

vol. 70, pp. 1803-1806, 2012.

35. T. Ohya, K. Nagatsu, H. Suzuki, M. Fukada, K. Minegishi, M. Hanyu, T. Fukumura and . M.-R. Zhang, "Efficient preparation of high-quality 64 Cu for routine use," *Nucl. Med. Biol.,* vol. 43, pp. 685-691, 2016.
36. D. McCarthy, R. Shefer, R. Klinkowstein, L. Bass, W. Margeneau, C. Cutler, C. Anderson and M. Welch, "Efficient production of high-specific-activity 64Cu using a biomedical cyclotron," *Nuclear Medicine and Biology,* vol. 24, pp. 35-43, 1997.
37. F. Szelecsényi, G. Blessing and S. Qaim, "Excitation functions of proton induced nuclear reactions on enriched 61Ni and 64Ni: possibility of production of No-carrier-added 61Cu and 64Cu at a small cyclotron," *Applied Radiation and Isotopes,* vol. 44, pp. 575-580, 1993.
38. A. Obata, S. Kasamatsu, D. McCarthy, M. Welch, H. Saji, Y. Yonekura and Y. Fujibayashi, "Production of therapeutic quantities of 64Cu using a 12 MeV cyclotron," *Nuclear Medicine and Biology,* vol. 30, pp. 535-539, 2003.
39. F. Poignant, S. Penfold, J. Asp, P. Takhar, P. Jackson , "GEANT4 simulation of cyclotron radioisotope production in a solid target,," *Physica Medica ,* vol. 32, p. 728–734 , 2016.
40. "Geant4 10.6 Release Notes," [Online]. Available: https://geant4-data.web.cern.ch/ReleaseNotes/ReleaseNotes4.10.6.html.
41. [Online]. Available: https://www.comecer.com/alceo-solid-target-processing-system.
42. W. Luo, M. Bobeica, D. Filipescu, I. Gheorghe , D. Niculae and D. Balabanski, "Production of radioisotopes of medical interest by photonuclear reaction using ELI-NP γ-ray beam," *Acta Physica Polonica B,* vol. 47, no. 3, 2016.
43. S. Agostinelli et al. , "Geant4 - a simulation toolkit," *Nucl. Instrum. Methods Phys. Res. A,* pp. 250-303, 2003.
44. W. Luo, M. Bobeica, I. Gheorghe, D. Filipescu, D. Niculae and D. Balabanski, "Estimates for production of radioisotopes of medical interest at Extreme Light Infrastructure – Nuclear Physics facility," *Appl. Phys. B,* 2016.
45. "Experimental Nuclear Reaction Data (EXFOR)," [Online]. Available: https://www-nds.iaea.org/exfor/.
46. C. K. Ross and T. Diamond, "Predictions regarding the supply of 99Mo and 99mTc when NRU ceases production in 2008," *Physics in Canada.*